Robust Estimation of Pharmacokinetic Modelling Parameters for the Analysis of Colorectal Tumours

L. N. Tanner[a], N. P. Hughes[a], N. Joshi[a], Sir Michael Brady[a], M. Anderson[b] and F. V. Gleeson[b]
[a]Department of Engineering Science, University of Oxford, Oxford, UK
[b]Department of Radiology, Churchill Hospital, Oxford Radcliffe Hospitals, UK

Abstract. Dynamic contrast-enhanced (DCE) MRI is a powerful tool for assessing tumour vasculature and for predicting patient response to therapy. DCE-MRI data can be quantified using pharmacokinetic models, allowing extraction of physiologically meaningful parameters. However, in clinical scans of rectal tumours many voxels within the tumour volume fail to produce valid pharmacokinetic parameters. By performing a sensitivity analysis, we find a high dependence of the model parameters on the pre-contrast relaxation time T_{10}. Estimation of T_{10} is sensitive to variations in the repetition time and to the effects of patient motion. We develop a new method for incorporating variations in TR into the parameter estimation process and combine it with non-rigid image registration. Our approach offers the potential for a substantial improvement in characterisation of rectal tumours.

1 Introduction

Colorectal cancer is the second largest cause of death from tumors in the world, with a global incidence of more than 1 million cases. The majority of patients diagnosed with stage II or stage III cancer currently undergo neoadjuvant chemoradiotherapy (CRT) prior to surgery. However, studies indicate that patients respond to therapy with widely varying degrees of success, with approximately 30% of tumours showing no response. In addition, 10% of patients show a complete response, such that there is no residual tumour present in the resected specimen. Unfortunately, since the treatment response can only be evaluated after surgery, these 'complete responders' undergo an unnecessary and highly invasive surgical procedure.

There is currently a great deal of interest in imaging to identify potential markers for predicting patient response. Of particular importance is dynamic contrast-enhanced MRI which is a widely used noninvasive technique for assessing tumour vasculature. Devries *et al.* [1] have demonstrated that primary rectal cancer response to CRT can be predicted by DCE-MRI using the perfusion index 'PI'. They argue that the uptake of contrast agent prior to therapy is indicative of the effectiveness of radiation therapy as it correlates with the presence of oxygen, known to influence radiosensitivity. Similarly, George *et al.* [2] suggest that DCE-MRI can be used as a surrogate marker for angiogenesis to predict and monitor response to treatment in patients with rectal cancer treated with preoperative CRT. It is generally thought that aggressive tumors tend to show greater contrast agent enhancement than less aggressive tumours [3]. Recent work however [4], suggests that simple DCE-MRI parameters correlate poorly with histological markers of angiogenesis and hypoxia, suggesting that DCE-MRI does not reflect a simple correlation with tissue vascularity in rectal cancer.

Our work is motivated by a prospective study of patients diagnosed with biopsy proven stage II or stage III rectal cancer. Patients in the study receive neoadjuvant radiotherapy with concurrent 5FU-based chemotherapy, which is followed by surgical resection. Each patient is imaged both pre- and post-therapy using dynamic contrast-enhanced (DCE) MRI, blood oxygen-level dependent (BOLD) MRI, and dynamic FDG-PET. The accurate quantification of DCE-MRI is one of the key challenges in assessing the likely patient response to therapy. In this paper we focus on the extraction of quantitative descriptors from DCE-MRI. We illustrate the issues involved in quantifying DCE-MRI parameters from rectal tumors, and show how the robustness of the analysis can be significantly improved by correcting for variations in repetition time (TR) and patient motion.

2 Dynamic Contrast Enhanced MRI Analysis

DCE-MRI involves intravenous injection of a paramagnetic contrast agent followed by acquisition of a series of T_1-weighted MRI images. The presence of contrast agent enables visualisation of the tumour vasculature. Since tumour vasculature is typically leaky with chaotic structure, the contrast agent arriving at the site of the tumour will, over a period of minutes move into and back out of the extravascular extracellular space (EES) surrounding the tumour. The tumour vasculature can then be quantified on a voxel-wise basis by fitting a pharmacokinetic model to the time intensity curve for each voxel. A standard approach for modelling DCE-MRI is the Tofts model [5], which has been applied extensively to the analysis and characterisation of many tumour types. The Tofts model is a two-compartment model, with separate compartments for the blood plasma and EES.

To fit the Tofts model it is necessary to first extract the contrast agent *concentration curve* for each voxel. The first step is to calculate at each voxel the signal enhancement curve $E(t) = S(t)/S(0) - 1$, where $S(t)$ is the MR signal value at time t and $S(0)$ is the baseline image acquired prior to the infusion of contrast agent. Unfortunately, the relationship between signal enhancement $E(t)$ and contrast agent concentration $C(t)$ is non-linear, and is dependent upon a number of factors including the sequence parameters and intrinsic properties of the tissue [6]. Of particular importance is the dependency on the pre-contrast relaxation time T_1, denoted T_{10}, which can vary for different voxels.

A standard approach for measuring T_{10} is to make use of variable flip angle gradient echo sequences. The gradient echo 3D pulse sequence is written as:

$$S = M_0 \sin\alpha \frac{1 - \exp(-\text{TR}/T_1)}{1 - \cos\alpha \exp(-\text{TR}/T_1)} \tag{1}$$

where S is the MR signal value, M_0 is the equilibrium longitudinal magnetisation, α is the flip angle and TR is the repetition time. With this approach, a series of n volumes are acquired with different flip angles. The choice of flip angle is critical, and is optimised for the expected T_1 range. Currently we acquire 4 volumes, with flip angles of $\alpha =$ 3, 9, 12 and 15 degrees. It is then possible to fit Eqn. 1 to the set of (S_n, α_n) pairs in order to extract the unknown parameters T_{10} and M_0 [7]. Given the estimated T_{10} value at each voxel we can then compute the contrast agent concentration $C(t)$ from the signal enhancement $E(t)$ using a look-up table approach [6].

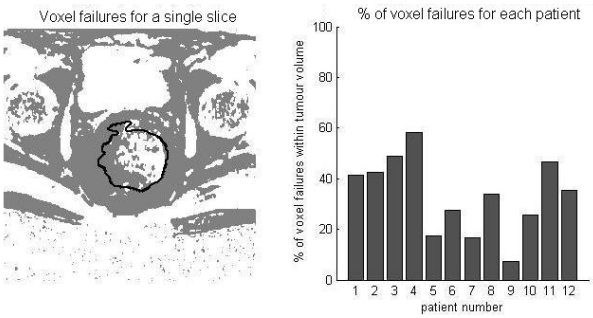

Figure 1. (a) Localisation of voxel failures for a single slice taken from patient 3. Gray values indicate failure in estimating $C(t)$ for that voxel. The tumour ROI is shown as a black outline. (b) The percentage of voxels that fail in the tumour volume for each patient.

3 Issues in pharmacokinetic modelling of DCE-MRI

The reliability with which the contrast agent concentration $C(t)$ can be estimated from the DCE-MRI data is one of the most significant factors in the pharmacokinetic modelling process. In particular voxel failures can occur when estimating $C(t)$ in the manner described above. A voxel failure occurs when the signal enhancement value $E(t)$ can not be mapped back to an equivalent gadolinium concentration value $C(t)$. This failure can occur when $E(t)$ is negative (corresponding to a *decrease* of the MR signal relative to the baseline), or when it is outside the permissable range determined by the T_{10} for that voxel. Negative enhancement values typically occur due to motion between the baseline image and the image acquired at time t, such that the signal values at a given voxel arise from different tissue locations. Similarly, out of bound values can arise when the estimated T_{10} value is affected by motion between the small flip angle images.

We observed that a high number of voxels were failing in our dataset, particularly at the boundary of the tumour region. Figure 1 illustrates the localisation of voxel failures within a typical slice, and the distribution of voxel failures within the whole tumour volumes[1] for our dataset of 12 patients. In section 6 we investigate the use of non-rigid registration techniques for addressing the issue of voxel failures in the estimation of contrast agent concentration.

4 Sensitivity of Pharmacokinetic parameters to variations in T_{10}

Even in the case where we can estimate a contrast agent concentration curve for a given voxel it is still possible that variations in T_{10} may give rise to unreliable estimates of the pharmacokinetic model parameters. The Tofts model is governed by two principle parameters, K^{trans} and k_{ep}, which characterise the uptake and washout of the contrast agent

[1] Tumour regions of interest (ROIs) were defined manually on each MRI slice by an experienced radiologist (MA).

at a given voxel. In order to better understand the reliability with which these two parameters can be computed, we performed a sensitivity analysis of the parameters to variation in T_{10}.

For T_{10} values in the range 200ms-1600ms (which correspond to the range of T_{10} values typically found in tissue [2]) we randomly sampled 100 (K^{trans}, k_{ep}) pairs and used the Tofts model to synthesise the corresponding concentration curve $C(t)$. K^{trans} was uniformly sampled from the range 0-1.8min^{-1} and k_{ep} was then randomly set to 2-5 times the sampled K^{trans} value [5]. Using the $C(t)$ and T_{10} values we calculated the corresponding signal enhancement $E(t)$. We then took 20 equally spaced values from the range $T_{10} \pm 100$ms and used $E(t)$ to estimate the 20 corresponding contrast agent curves $\tilde{C}_i(t)$ to which we fitted the Tofts model. We compared the resulting 20 ($\tilde{K}^{\text{trans}}$, $\tilde{k}_{\text{ep}}$) pairs with the original (K^{trans}, k_{ep}) pair. For each T_{10} we calculated the average error. The results are shown in figure 2(a) which illustrates that, particularly for low T_{10}, K^{trans} is highly dependent upon accurate estimation of T_{10}.

In DCE-MRI analysis, errors in T_{10} may arise in two possible ways. Firstly, due to variations in the repetition time (TR) that are not taken into account during the analysis, and secondly due to noise and motion between the small flip angle images. We now consider strategies for addressing both these issues.

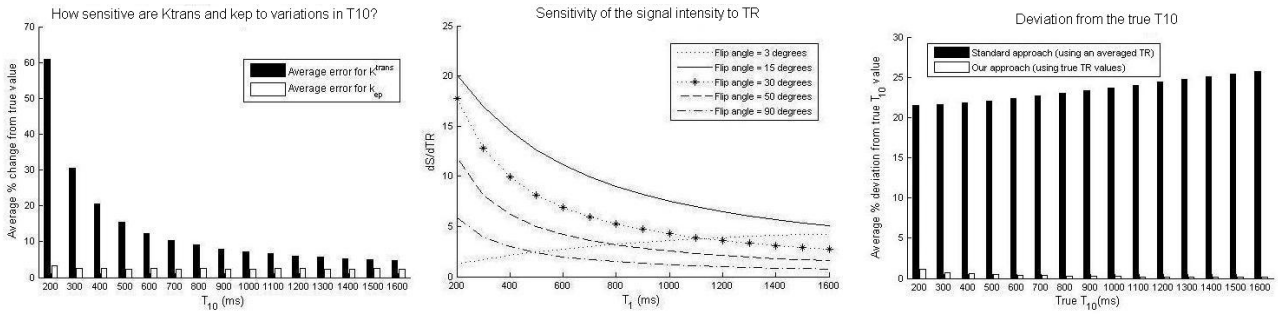

Figure 2. (a)Dependence of pharmacokinetic parameters on variation in T_{10}. For each T_{10} we use the Tofts to simulate 100 SE curves from different (K^{trans},k_{ep}) pairs. We vary T_{10} by 100ms and recalculate the (K^{trans},k_{ep}) parameters. Bars illustrate the average percentage change from the original value. (b) The dependence of the image signal on the repetition time. Each curve illustrates the derivative of S with respect to TR for a different flip angle. We set M_0 to 1200 as per [6]. (c) Error in T_{10} estimation. We simulated small flip angle signals using variable TR values. Black bars shows the mean error using the standard method with an average TR. White bars show the mean error using the new method with variable TR values.

5 Correcting for variations in TR

In a clinical setting, the small flip angle sequences are often performed with variable TR values due to intricacies of the MRI software. In our dataset, TR values for the small flip angle images are in the range $2.5 - 5.5$ms with one TR used for the smallest two flip angles, and a second for the larger two flip angle sequences. The standard method typically used for calculating T_{10} from variable flip angle images assumes that TR is constant [7]. To gain a better understanding of the variation in the MR signal with variation in TR, we first differentiated the MR signal equation (Eqn. 1) w.r.t TR:

$$\frac{dS}{d\text{TR}} = M_0 \sin\alpha \frac{\frac{1}{T_1}\exp(-\text{TR}/T_1)(1-\cos\alpha)}{(1-\cos\alpha\exp(-\text{TR}/T_1))^2} \tag{2}$$

Figure 2(b) illustrates the derivative of the signal S with respect to TR for different flip angles. For $\alpha \approx 15$ degrees, small variations in TR can cause large changes in the signal. Therefore, rather than assuming an average TR value, we wish to incorporate the true TR values into our calculation of T_{10}.

5.1 Incorporating Multiple TR values

As previously discussed in section 2 we can calculate T_{10} by rearranging Eqn. 1 in the form of a linear regression and fitting this to the set of (S_n, α_n) pairs at each voxel [7]. The linear regression takes the following form:

$$\frac{S}{\sin\alpha} = exp(-\text{TR}/T_1)\frac{S}{\tan\alpha} + M_0(1-exp(-\text{TR}/T_1)) \tag{3}$$

with the gradient given by $m = exp(-\text{TR}/T_1)$ and the intercept given by $M_0(1-exp(-\text{TR}/T_1))$. This allows T_1 to be computed as $-\text{TR}/\ln(m)$, requiring however that TR be constant for all n low flip angle image sequences.

We can allow for variations in TR for different flip angle images by observing that for small $-\text{TR}/T_1$ we have the following approximation: $\exp(-\text{TR}/T_1) \approx 1 - \text{TR}/T_1$. Substituting this approximation into Eqn. 1 and rearranging in the form of a linear regression we have:

$$\frac{S}{\text{TR}}\left(\frac{1}{\sin\alpha} - \frac{1}{\tan\alpha}\right) = -\frac{1}{T_1}\frac{S}{\tan\alpha} + \frac{M_0}{T_1} \tag{4}$$

where the gradient m is given by $-1/T_1$ and the intercept c by M_0/T_1. We can then fit Eqn. 4 to a set of (S_n, α_n, TR_n) triplets and compute T_1 from the gradient m by $T_1 = -1/m$.

We evaluated our approach by first sampling T_{10} in the manner previously described in section 3. Next, we uniformly sampled 25 pairs of TR values from the range $2.5 - 5.5$. We calculated the MR signal S for the flip angles $\alpha = 3, 9, 12$ and 15 degrees, using the smaller TR for the first two flip angles, and the larger TR for the latter two. We then used the standard approach (as given by Eqn. 3) and our new approach to estimate T_{10}. In the case of the standard approach we used the average TR value of the sampled pair. We recorded the percentage change in both estimates from the true value.

The results of this simulation are shown in figure 2(c). With the standard approach (using an averaged value of TR) the average percentage error in the estimated T_{10} is between 20-25%. This can be explained by the analysis in the previous section which showed high values of the derivative $dS/d\text{TR}$ for flip angles close to $\alpha = 15$. Conversely the new approach (which takes into account variations in TR) results in a significantly more accurate estimation of T_{10}. Thus by incorporating variations in TR into the estimation of T_{10} we can greatly improve the robustness of the pharmacokinetic parameters.

6 Registration

Voxel-wise pharmacokinetic analysis depends strongly on the assumption that the signal from each voxel arises from a specific spatial location in the tissue throughout the duration of the scan. In non-rigid organs such as the colorectum, the compressive nature of the tissue can result in non-uniform displacements. As a consequence, signal values at a given voxel can arise from different tissue locations. This problem is most pronounced at tissue boundaries and in highly heterogeneous tumour regions where there is significant variation in the MR signal. As discussed in section 3 uncorrected patient motion plays a significant role in pharmacokinetic modelling errors.

To overcome this issue, we registered both the DCE-MRI and the small flip angle images using Rueckert's freeform deformation approach [8]. In order to incorporate variations in image intensity due to contrast agent, we used Normalised Mutual Information as a similarity measure, which maximises the amount of shared information between images.

The images were acquired during the same imaging session and so the MR scanners coordinate frame was used for initialisation of the registration. The images are registered to a reference image. In the case of DCE-MRI we use the baseline image acquired prior to contrast agent injection. For the small low angle images we use the sequence with flip angle $\alpha = 3$. We began by applying a rigid registration algorithm, removing large rigid translations and rotations. Visual inspection of the data sets revealed that there were still residual non-rigid deformations within the tumour volume.

Following rigid registration we performed non-rigid registration within a 3D volume encompassing the ROI. The non-rigid registration is run to convergence three times using an increasingly fine control point mesh. The initial transformation aims to capture the larger scale differences between the images. The control point spacing determines the amount of motion that can be corrected, and at the finest resolution is chosen to match the image resolution. At each level the image is blurred with an increasingly fine Gaussian filter.

7 Results

Our objective is improvement in the reliability of pharmacokinetic modelling parameters, through motion correction and by accounting for variations in TR during T_{10} estimation. In order to determine the effect of the registration on the pharmacokinetic modelling, we computed the percentage of voxel failures (as previously described in section 3) both before and after registration. Figure 3(a) demonstrates that with our approach we can see a significant reduction in voxel failures within the tumour volumes for the patients in our data set. Figure 3(b) illustrates the original K^{trans} parametric map acquired for one typical patient with the parametric map calculated after accounting for multiple TR values and motion correction. There is a marked difference in K^{trans} values as a result of our adjustments.

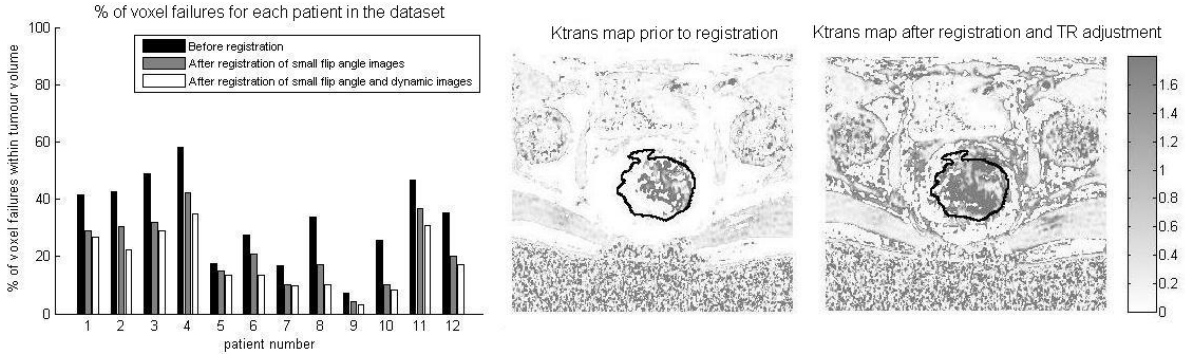

Figure 3. (a)The percentage of voxels that fail in the tumour volume (i) before registration, (ii) after registration of small flip angle images with correction for multiple TR, and (iii) after also incorporating registration of DCE-MRI images. A typical K^{trans} map taken from one patient (b) before registration and (c) after registration of both DCE-MRI and small flip angle images, and allowing for multiple TR.

8 Discussion

Our current work is focused on building predictive models of patient treatment response using a suitable description of the pharmacokinetic parameters evaluated from DCE-MRI. Most quantitative analysis of rectal tumours involves calculating the mean or median K^{trans}, reducing the effects of noise and motion. Registering both the low flip angle images used to estimate T_{10} and the DCE-MRI images, as well as properly accounting for variations in TR, leads to a significantly more robust analysis (as assessed by the reduction in the number of voxel failures), which is imperative for voxel-wise analysis. The residual voxel failures are a result of imperfections in image registration, partial volume effects at the tumour boundary and small differences in the orientation of the MR imaging planes used for the different MR sequences. We plan to address these issues in our future work. Whilst it is not possible to measure the true K^{trans} value, the ultimate assessment of our results will be the accuracy with which we can predict patient response to therapy.

We contend that the heterogeneity of a tumour provides valuable information on the pathology of the tissue's microenvironment. Fusion of DCE-MRI images with BOLD-MRI and PET provides information on the tissue's glucose metabolism, perfusion and oxygenation. Imaging features from each modality will be used to separate patients into biologically realistic groups, for example those with a marked decrease in metabolic activity. We plan to characterise the tumour phenotype from these imaging modalities by computing a "signature" that will quantify the heterogeneity of the tumour microenvironment, and the variation between patients. The combination of these ideas will allow us to consider the relationship between the tumour microenvironment, the parameters that arise from imaging it and the value functional imaging techniques may afford.

We thank Julia Schnabel from the Institute for Biomedical Engineering in Oxford for her advice on image registration.

References

1. A. de Vries *et al.* "Monitoring of tumor microcirculation during fractionated radiation therapy in patients with rectal carcinoma." *Radiology* **217**, pp. 385–391, 2000.
2. M. George *et al.* "Non-invasive methods of assessing angiogenesis and their value in predicting response to treatment in colorectal cancer." *Br J Surg* **88**, pp. 1628–1636, 2001.
3. N. Tuncbilek *et al.* "Use of dynamic contrast-enhanced magnetic resonance imaging for differentiating between aggressive rectal tumours." *Hong Kong Med J* **12**, pp. 480–482, 2006.
4. G. Atkin *et al.* "Dynamic contrast-enhanced magnetic resonance imaging is a poor measure of rectal cancer angiogenesis." *Br J Surg* **93**, pp. 992–1000, 2006.
5. P. Tofts. "Modeling tracer kinetics in dynamic Gd-DTPA MR imaging." *JMRI* **7**, pp. 91–101, 1997.
6. P. Armitage *et al.* "Extracting and visualizing physiological parameters using dynamic contrast-enhanced magnetic resonance imaging of the breast." *Medical Image Analysis* **9**, pp. 315–329, 2005.
7. S. Deoni *et al.* "Rapid combined T_1 and T_2 mapping using gradient recalled acquisition in the steady state." *Magnetic Resonance in Medicine* **49**, pp. 515–526, 2003.
8. D. Rueckert *et al.* "Non-rigid registration using free-form deformations: Application to breast MR images." *IEEE Trans Med Imaging* **18**, pp. 712–721, 1999.